Eur. Phys. J. Appl. Phys. **56**, 30301 (2011)
DOI: 10.1051/epjap/2011100463

THE EUROPEAN PHYSICAL JOURNAL
APPLIED PHYSICS

Regular Article

p-Type transparent conducting copper-strontium oxide thin films for optoelectronic devices

H.A. Mohamed[a]

Physics Department, Faculty of Science, Sohag University, 82524 Sohag, Egypt
Physics Department, Teachers College, King Saud University, 11148 Riyadh, Kingdom of Saudi Arabia

Received: 20 November 2010 / Received in final form: 2 March 2011 / Accepted: 1 August 2011
Published online: 14 November 2011 –

Abstract. *p*-Type thin films of copper-strontium oxide (Cu-Sr-O) have been deposited by e-beam evaporation technique on microscopic glass substrates. A study of optical, electrical and structural properties was performed on the thin films, varying temperature of annealing. Amorphous Cu-Sr-O films were obtained at low temperature. Partially polycrystalline films were obtained at high temperature of 550 °C with transparency over 72% at wavelength from 600 to 700 nm in the visible region and 83% in the near infrared region (λ = 1800:2500 nm). The optical band gap was estimated to be ∼3.5 eV. The Seebeck coefficient measurements showed that the as-deposited films represented *n*-type conduction and with annealing temperature these films converted to *p*-type. The electrical conductivity measurements at room temperature of annealed films at temperature of 550 °C represented the best value about 2 S/cm. The other optical parameters such as refractive index, extinction coefficient, dielectric constant and cutoff wavelength were studied as a function of annealing temperature.

1 Introduction

Transparent conducting oxides (TCOs) have many applications in several optoelectronic devices such as light-emitting diodes (LEDs), solar cells, and flat panels as well as flexible displays [1–3]. Although the TCOs have a vast range of applications as mentioned above, very little work has been done on active device fabrication using TCOs [4,5]. This is because most of the aforementioned TCOs are *n*-type semiconductors. But the corresponding *p*-type transparent conducting oxides (*p*-TCOs), which are essential for junction devices, were surprisingly missing in thin film form for a long time until in 1997, Kawazoe et al. reported *p*-type conductivity in a highly transparent thin film of copper aluminum oxide [6]. This has opened up a new field in optoelectronics device technology, the so-called "Transparent Electronics" or "Invisible Electronics" [7], where a combination of the two types of TCOs in the form of a *p*-*n* junction could lead to a "functional" window, which transmits visible portion of solar radiation yet generating electricity by the absorption of the UV part [6].

Most of the *p*-type transparent conducting materials are Cu and Ag based. However, the optical and electrical properties of these materials are still lower than those obtained for *n*-type TCOs materials. For example, the transmittance and conductivity for $CuAlO_2$ films with thickness 230 nm are about 70% and 0.34 S cm^{-1} respectively [8], the $CuCrO_2$ films with thickness 250 nm have transmittance 40% and conductivity 1 S cm^{-1} [9], the $CuCr_{1-x}Mg_xO_2$ with thickness 270 nm have transmittance 50% and conductivity 220 S cm^{-1} [6], and for $AgCoO_2$ films with thickness 150 nm have a transmittance 50% and conductivity about 0.2 S cm^{-1} [10]. Now for diverse device applications, it is of utmost importance to prepare various types of *p*-TCOs with superior optical and electrical characteristics, at least comparable to those of the existing, widely used *n*-TCOs, which have a transparency above 80% in the visible region and a conductivity about 1000 S cm^{-1} or more.

In this work, the effect of heat treatment on the structural, optical, and electrical properties of Cu-Sr-O thin films prepared by electron beam evaporation technique has been studied. A compromise between low resistivity and high transmission of light has been made in order to examine the quality of films as transparent-conductive ones.

2 Experimental details

Bulk Cu-Sr-O targets were prepared using SrO powder (99.999% purity) and CuO powder (99.99% purity) materials. The powder was pressed using cold pressing technique to form the pellets of mixture weight ratio for CuO_{91}:SrO_9, which were sintered at 900 °C for 5 h and then cooled slowly to room temperature in a fully controlled furnace in air. Sintering process assists to produce

[a] e-mail: hussein_abdelhafez2000@yahoo.com

lumps of powder materials in a bulky form without affecting their chemical properties, while their physical properties approach those of single crystal phase [11,12]. The sintering process is usually carried out in the temperature range $\frac{T_M}{2} \leq T \leq T_M$, where T_M is the melting point of the material to be sintered [13]. The electron beam evaporation was used to deposit the prepared Cu-Sr-O tablets into ultrasonically cleaned microscopic slides with dimensions of 1 cm × 2.5 cm. Edwards high vacuum (2×10^{-5} torr) coating unite model E306A was used for this purpose. The rate of deposition and the thickness of the films were controlled to be about 10 nm min^{-1} and 110–120 nm, respectively, by means of a digital film thickness monitor model TM200 Maxtek. Optical measurements (transmittance T and reflectance R) were performed using a Jasco V-570 UV-VIS-NIR spectrophotometer in the wavelength range from 200 to 2500 nm at normal incidence. Structural analysis of as-deposited and annealed films was carried out on Phillips (PW-1710) Cu Kα diffractometer ($\lambda = 1.541838$ Å) by varying diffraction angle 2θ from 4 to 80 by step width of 0.04 in order to evaluate crystalline phase and crystallite orientation. The electrical resistivity measurements were carried out using a two-terminal configuration by applying a constant voltage (≈5 V) to the sample and measuring the current through it using a Keithley 614 electrometer. The measurements were done at room temperature. Electrical contacts were made by applying silver paste over the surface of the films with a separation of 3 mm. Applying the temperature difference between the two film electrodes, the Seebeck coefficient (S) measurements were carried out for Cu-Sr-O films at room temperature and at annealing temperature of 300–550 °C.

3 Results and discussion

3.1 Structural characterization

Figure 1 shows X-ray diffraction (XRD) results of Cu-Sr-O films annealed at various temperatures (as-550 °C). The as-deposited films and the annealed films at low temperature exhibit a partially amorphous structure with some small peaks belonging to Cu_2SrO_2 (1 0 3), $CuSrO_2$ (0 8 0) and SrO_2 (0 0 2) plane. The films that annealed at 450 and 550 °C represent the same above peaks with an increasing intensity of some peaks such as SrO_2 (0 0 2) and Cu_2SrO_2 (1 0 3). Moreover, no preferred orientations were observed even at high temperature. From this figure it is evident that the annealing at high temperature seemed to improve the film crystallinity.

3.2 Optical and electrical properties

Figure 2 illustrates the transmission and reflection spectra of Cu-Sr-O thin films deposited at room temperature (as-prepared) and annealed in air at various temperatures (300, 400, 450, 500 and 550 °C) for 2 h. It was seen from the transmission spectra that the as-deposited films are

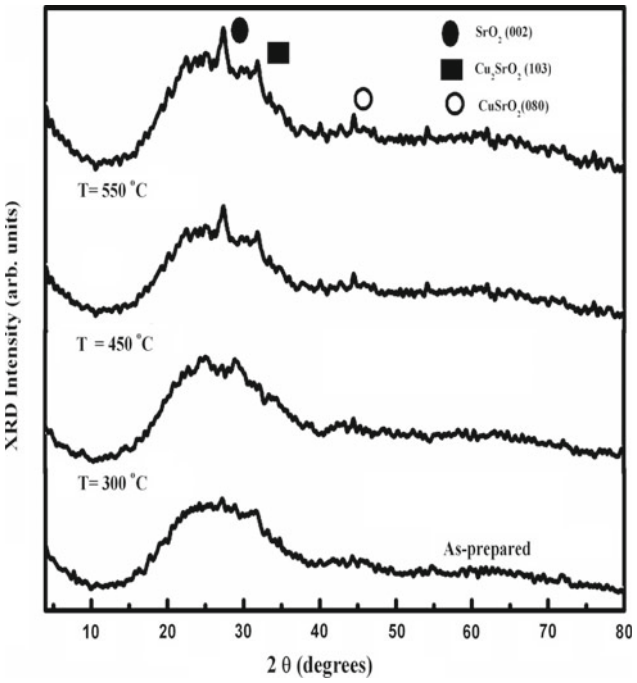

Fig. 1. XRD patterns of Cu-Sr-O thin films deposited on glass substrate at room temperature and followed by annealing in air at temperature of 300, 450 and 550 °C.

opaque since their transmission is less than 10% in the visible region ($\lambda = 380$:800 nm). The reflection of as-deposited films records high value about 50% in near infrared region ($\lambda = 1800$:2500 nm). This behavior of transmission and reflection of as-deposited films can be attributed to the oxygen deficiency [14]. In addition, the as-deposited films represent high free carrier concentration (as will be seen in Tab. 1) which can lead to a narrowing of the band gap due to carrier-carrier and carrier-impurity interactions [15]. On the other hand, with increasing the temperature the transmission increases and the reflection decreases due to the substitution of oxygen during annealing process in air. Figure 2a shows that the absorption edge of annealed Cu-Sr-O films appears to be shifted toward the shorter wavelength side. The films annealed at 550 °C show an average transmittance of 72% at spectral range 600–700 nm of wavelength in the visible region and 83% in the near infrared region ($\lambda = 1800$:2500 nm). These results are considered better than those obtained in references [6,9].

The absorption coefficient α of Cu-Sr-O films was calculated from the transmittance T and reflection R spectra using the equation [12]:

$$\alpha = \frac{2.303}{d} \log_{10}\left(\frac{1-R}{T}\right), \quad (1)$$

where d is the film thickness. As shown from Figure 3 the absorption coefficient is found to be about 10^4 cm^{-1}, which exponentially decreases as both wavelength and annealing temperature increase. Besides, the decrease in absorption coefficient indicates a decrease in optical density of Cu-Sr-O films since the absorption coefficient is directly

Table 1. The refractive index at wavelength 550 nm (n_{550}), free carrier concentration per effective mass (N/m^*), electrical resistivity (ρ), figure of merit (Φ), and the Seebeck coefficient (S) of Cu-Sr-O thin films prepared at room temperature and followed by annealing in air at different temperatures.

T (°C)	As	300	400	450	500	550
n_{550}	3.12	2.9	2.31	2.3	2	2.14
N/m^* ($\mathrm{cm^{-3}\ g^{-1}}$)	2×10^{47}	4.79×10^{46}	4.64×10^{46}	3.8×10^{46}	3×10^{46}	2.67×10^{46}
ρ (Ω cm)	5.6×10^{-5}	8.8×10^{1}	4.1×10^{1}	3.8×10^{1}	2.6×10^{1}	5×10^{-1}
Φ ($\Omega^{-1}\,\mathrm{cm^{-1}}$)	–	0.55	1.21	.144	2.16	134.2
S (μV/K)	−61.8	177.2	182.4	189.6	209.1	226.5

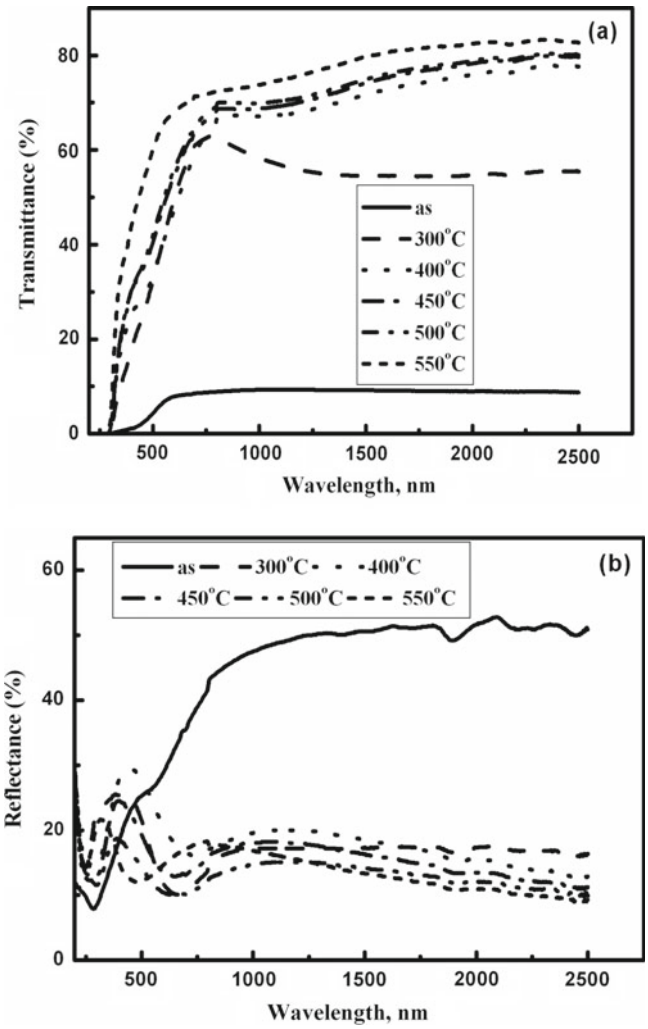

Fig. 2. Transmission and reflection spectra of as-deposited and annealed Cu-Sr-O films as a function of wavelength at different temperatures.

proportional to the optical density as reported in some articles [16–18].

Electronic band structure calculation done by Nie et al. [19] and Ohta et al. [20] has demonstrated a direct band gap transition for Cu-Sr-O thin films. In this circumstance the absorption coefficient α can be related to the photon energy $h\nu$ by

$$(\alpha h\nu)^2 = A\,(h\nu - E_g)\,, \qquad (2)$$

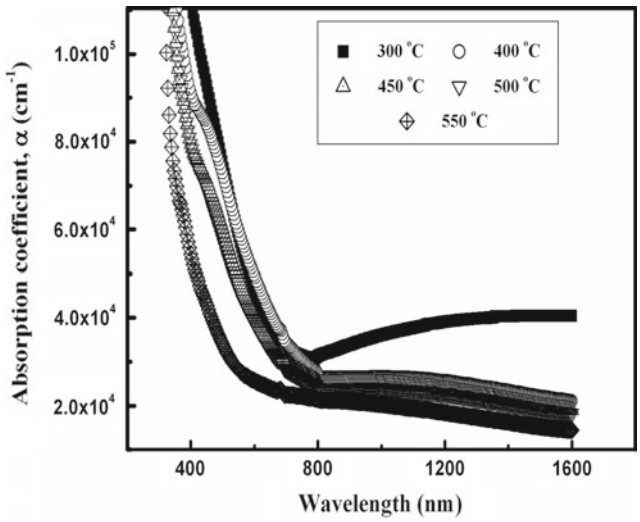

Fig. 3. Variation optical absorption coefficient of Cu-Sr-O films with wavelength at different values of annealing temperature.

where A is a constant, $h\nu$ is the photon energy and E_g is the optical energy gap. A plot of $(\alpha h\nu)^2$ vs. the photon energy ($h\nu$) is displayed in Figure 4a for the films annealed at 300, 400, 450, 500 and 550 °C. The estimated direct optical energy gap as a function of annealing temperature for Cu-Sr-O films is plotted in Figure 4b. It was found that the optical energy gap of these films increases with increase of annealing temperature, indicating that the annealing temperature in air is considered a significant tool to improve the film transmission. The energy gap values of Cu-Sr-O films annealed at temperature of 300, 400, 450, 500 and 550 °C were calculated as 3.3, 3.44, 3.46, 3.46 and 3.53 eV. On the other hand, due to the poor transmittance and undistinguishable absorption edge the optical energy gap of the as-deposited films could not be estimated in this work. The increase in energy gap with temperature may be due to the decrease in free carrier concentration or to the improvement in film crystallinity as seen in Figure 1 [12]. Besides, it is observed that the cutoff wavelength (see Fig. 4b) has been shifted toward ultraviolet region (high energy) with the increase in annealing temperature. This behavior was observed for fundamental absorption edge as shown in Figure 2a since the cutoff wavelength is directly affected by the energy gap of the material as reported by Knickerbocker and Kulkarni [21].

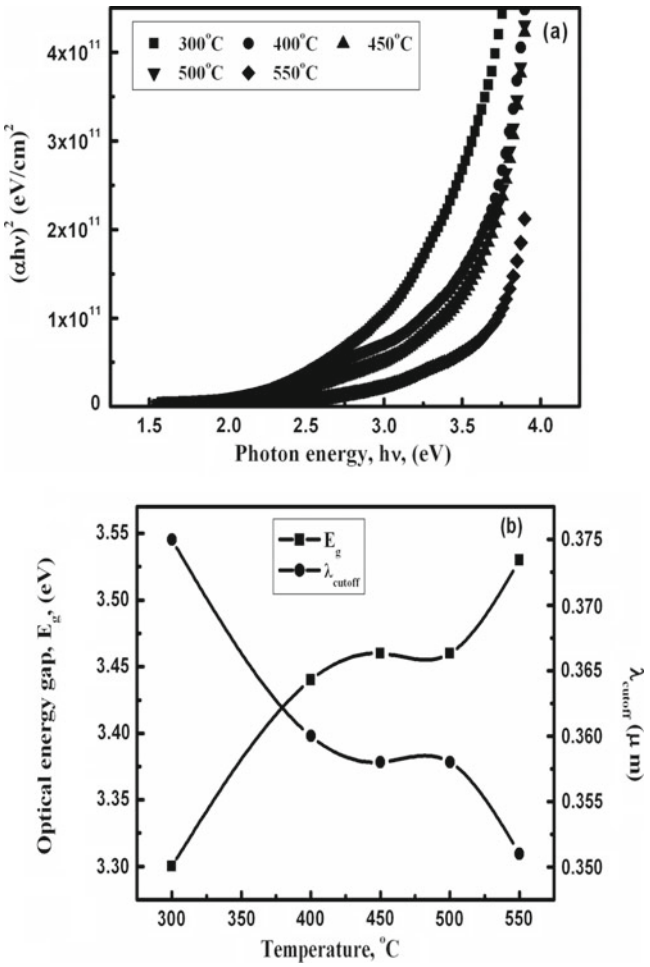

Fig. 4. (a) $(\alpha h\nu)^2$ vs. $h\nu$ and (b) optical energy gap and λ_{cutoff} at different temperatures of Cu-Sr-O films.

The spectral refractive index (n) and extinction coefficient (K) of the Cu-Sr-O films were calculated from the transmittance (T) and reflection (R) spectra using the equations [22]:

$$n = \frac{1+R}{1-R} \pm \left[\left(\frac{R+1}{R-1} \right)^2 - \left(1 + k^2\right) \right]^{1/2}, \quad (3)$$

$$K = \frac{2.303}{4\pi} \frac{\lambda}{d} \log_{10} \left(\frac{1-R}{T} \right). \quad (4)$$

The dispersion of n with wavelength (λ) is plotted in Figure 5 at different values of temperature. It is clear that the dependence of the refractive index on temperature does not show a clear behavior. Therefore, the values of refractive index at $\lambda = 550$ nm were calculated and are listed in Table 1. As result of this table, the refractive index decreases with the increase of annealing temperature. The decrease in the refractive index with temperature may be due to the decrease in optical density of Cu-Sr-O films as mentioned above in discussing Figure 3 and/or the increase in energy gap as observed from Figure 4b as reported in some references [23,24]. On the other hand, it could be concluded from equation (4) that the extinction

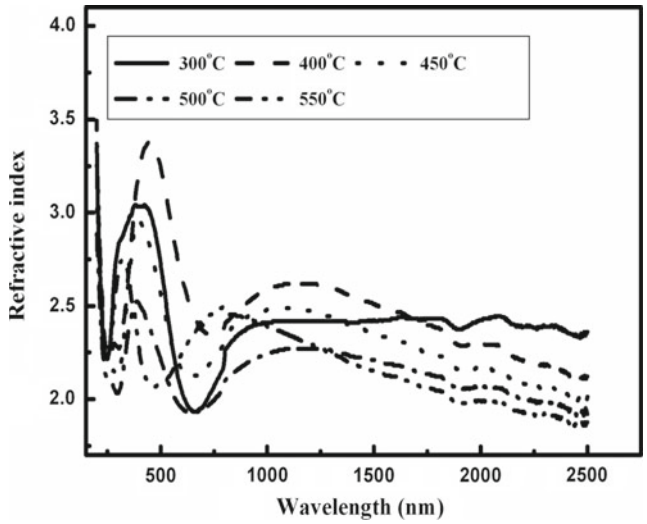

Fig. 5. Variation of refractive index with wavelength of annealed Cu-Sr-O films at different temperatures.

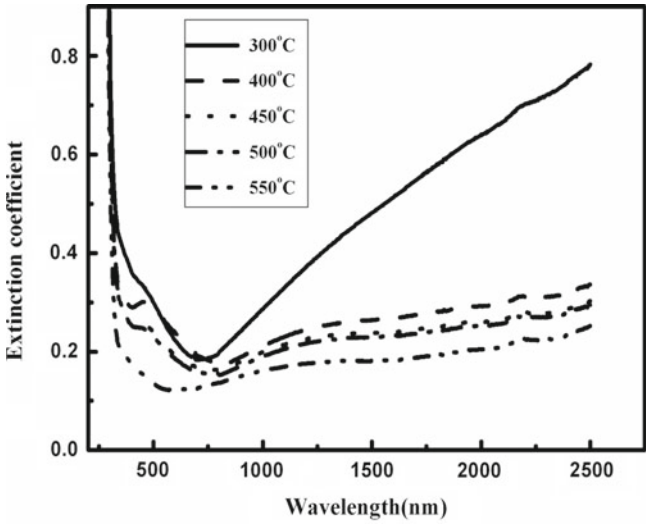

Fig. 6. Variation of extinction coefficient with wavelength of annealed Cu-Sr-O films at different temperatures.

coefficient (K) is inversely proportional to the film transmission. Hence, the extinction coefficient decreases with increasing the temperature as shown in Figure 6.

For further analysis of the optical data a number of useful, associated relations can be derived to link the real and imaginary parts of the dielectric function and the optical constants (n, k). The following relations have been used to calculate the values of the real part (ε') and imaginary part (ε'') of the dielectric constant for Cu-Sr-O films:

$$\varepsilon' = n^2 - k^2 = \varepsilon_i - \frac{e^2}{4\pi^2 c^2 \varepsilon_0} \left(\frac{N}{m^*} \right) \lambda^2, \quad \varepsilon'' = 2nk, \quad (5)$$

where ε_i is the infinity high frequency dielectric constant, e is the elementary charge, c is the light velocity, ε_0 is the permittivity of free space, N is the optical free carrier concentration, m^* is the effective mass and λ is the light wavelength.

The variation of the real part (ε') and imaginary part (ε'') of the dielectric constant with wavelength at different temperatures is shown in Figures 7 and 8. It can be seen from these figures that the real part of the dielectric constant decreases with increasing the wavelength but the imaginary part increases. The values of real part are higher than those of imaginary part. In addition, both the real and imaginary parts of the dielectric constant decrease with increasing the temperature due to the decrease of refractive index and extinction coefficient with temperature as shown in Figures 5 and 6. It is known that the imaginary part of the dielectric constant is directly related to the density of states within the forbidden gap of thin film materials [25]. Therefore, this decrease in ε'' with annealing temperature leads to decreasing the density of states within the forbidden gap and then increase in the energy gap as shown in Figure 4b. From the slope and intercept of the plotted curves in Figure 7, two important parameters namely free carrier concentration (N) and infinity high frequency dielectric constant or the residual dielectric constant (ε_i) can be determined. The values of free carrier concentration per effective mass were calculated and are listed in Table 1. It can be seen that the values of N/m^* and hence N decrease with further increase in temperature and the high variation of these values (one order of magnitude) occurred between as-deposited films and the films that annealed at 300 °C, indicating that the as-deposited films have high free carriers which leads to degrading the optical transmittance of these materials as seen in Figure 2a. The estimated values of infinity high frequency dielectric constant (ε_i) are plotted in Figure 7b as a function of temperature. It can be seen that this parameter exponentially decreases as the temperature increases. The as-deposited films have the maximum value about 42 and the other values ranged between 6.6 and 4.6 in the temperature range 300–550 °C.

The electrical resistivity ρ of Cu-Sr-O films was measured at room temperature for as-deposited and annealed films at different temperatures. The obtained values are listed in Table 1. It is expected that the as-deposited films have high conductivity due to the oxygen deficiency, which happened during the deposition process. Apart from the as-deposited films, it is observed that the electrical resistivity of Cu-Sr-O films decreases with increasing the annealing temperature. The lowest resistivity value obtained at 550 °C was about $5 \times 10^{-1}\,\Omega$ cm. Although, the free carrier concentration decreases with temperature the electrical resistivity decreases also. This behavior may be due to the increase in mobility with annealing temperature since the films' crystallinity seemed to improve at high temperature.

The Seebeck coefficient (S) measurements for Cu-Sr-O films were taken into account to determine the type of these films. The dependence of S on temperature was measured and is listed in Table 1. It is clear that, the as-deposited films exhibit negative sign of S that means as-deposited Cu-Sr-O films represent *n*-type conduction. With increasing the annealing temperature the sign of S changed to positive and its value increases.

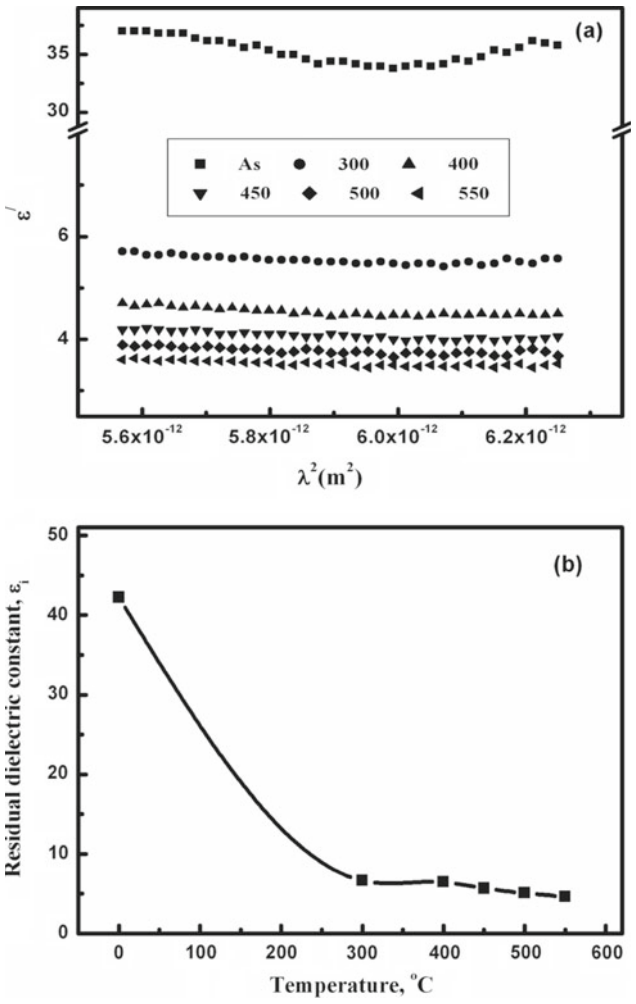

Fig. 7. (a) Plot of the real part of dielectric constant (ε') as a function of wavelength (λ^2) and (b) the residual dielectric constant (ε_i) of Cu-Sr-O films at different temperatures.

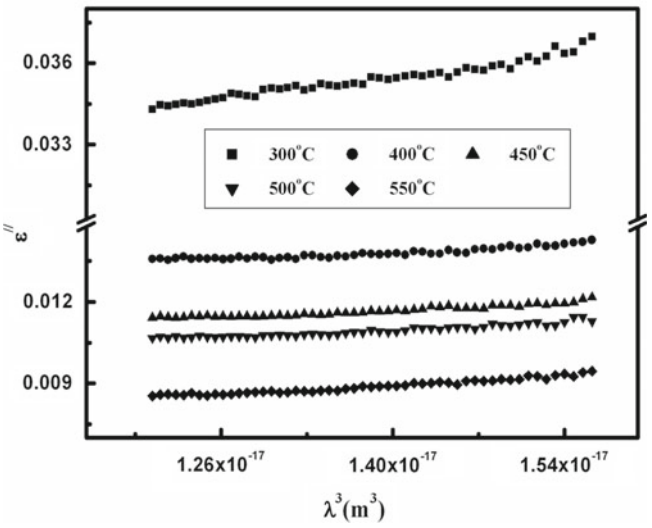

Fig. 8. Plot of the imaginary part of dielectric constant (ε'') as a function of λ^3 of annealed Cu-Sr-O films at different temperatures.

Table 2. Comparison of some optical and electrical parameters (transmittance in visible region T_{vis}, energy gap E_g and electrical conductivity σ) that were studied in this work with other work.

p-Type thin films	T_{vis} (%)	E_g (eV)	σ (S/cm)	T (°C)	References
Cu-Sr-O	72	3.53	2	550	Current work
Cu-Sr-O	<60	–	2×10^{-3}	550	[27]
Cu-Sr-O	>60	3.12	5.3×10	250	[28]
CuCrMgO	40	3.1	1	–	[9]
Cu-Al-O	70	3.5	0.34	–	[4]
$AgCoO_2$	50	4.15	0.2	400	[10]
Sn-Sb-O	65–80	3.4–3.5	6	700	[29]

3.3 Figure of merit

The quality of a transparent conducting oxide will be judged by the parameter of figure of merit Φ. The figure of merit of the film was calculated from the optical transmittance and sheet resistance data using the equation [26]:

$$\phi = \frac{T}{\rho}, \tag{6}$$

where T is the average transmittance in visible region (320–800 nm) and ρ (Ω cm) is the electrical resistivity at room temperature. Results of figure of merit are calculated and listed in Table 1. The figure of merit allows us to quantify film quality and to confirm that the Cu-Sr-O films annealed at temperature of 550 °C resulting in the best films. The figure of merit of as-deposited films was not taken into account.

Finally, Table 2 represents a comparison of some optical and electrical parameters such as transmittance in visible region (T_{vis}), optical energy gap (E_g) and electrical conductivity (σ) that were studied in this work with other literature.

4 Conclusions

Copper-strontium oxide thin films were deposited on glass substrates by e-beam technique. The prepared films show good optical quality with transmittance over 72% at wavelength range 600:700 nm in the visible region. The energy gap of copper-strontium oxide represents direct allowed transition with value of 3.53 eV for the annealed films at 550 °C. X-ray diffraction measurements revealed an amorphous structure with some small peaks of as-deposited and annealed films at low temperature. The annealing at high temperature seemed to improve the film crystallinity. The electrical resistivity of the annealed films was studied at room temperatures. The minimum resistivity values of 5×10^{-1} (Ω cm) were obtained for annealed film at 550 °C. The figure of merit confirms that the Cu-Sr-O films annealed at temperature of 550 °C resulting in the best films as transparent conducting p-type. It was observed that the refractive index, extinction coefficient and dielectric constant were affected by annealing temperature.

The author would like to thank the Program Research Center at College of Teachers, Deanship of Scientific Research, King Saud University, Riyadh, Saudi Arabia, for funding and supporting this research.

References

1. J. Lee, J. Metson, P.J. Evans, R. Kinsey, D. Bhattacharyya, Appl. Surf. Sci. **253**, 4317 (2007)
2. G. Akhlesh, A.D. Compaan, Appl. Phys. Lett. **85**, 684 (2004)
3. O. Bamiduro, H. Mundle, R.B. Konda, A.K. Pradhan, Appl. Phys. Lett. **90**, 252108 (2007)
4. C.H. Seager, D.C. McIntyre, W.L. Warren, B.A. Tuttle, Appl. Phys. Lett. **68**, 2660 (1996)
5. M.W.J. Prince, K.O. Gross-Holtz, G. Muller, J.B. Cillessen, J.B. Giesbers, R.P. Weening, R.M. Wolf, Appl. Phys. Lett. **68**, 3650 (1996)
6. H. Kawazoe, M. Yasukawa, H. Hyodo, M. Kurita, H. Yanagi, H. Hosono, Nature **389**, 939 (1997)
7. G. Thomas, Nature **389**, 907 (1997)
8. H. Yanagi, S. Inoue, K. Ueda, H. Kawazoe, H. Hosono, N. Hamada, J. Appl. Phys. **88**, 4159 (2000)
9. R. Nagarajan, A.D. Draeseke, A.W. Sleight, J. Tate, J. Appl. Phys. **89**, 8022 (2001)
10. J. Tate, M.K. Jayaraj, A.D. Draeseke, T. Ulbrich, A.W. Sleight, K.A. Vanaja, R. Nagarajan, J.F. Wager, R.L. Hoffman, Thin Solid Films **411**, 119 (2002)
11. W.D. Kingery, in *Kinetics of High Temperature Process*, edited by W. Kingery (MIT Press, Cambridge, MA, 1959), p. 187
12. H.A. Mohamed, J. Phys. D: Appl. Phys. **40**, 4234 (2007)
13. H.A. Mohamed, Optoelectron. Adv. Mater.-Rapid Commun. **3**, 693 (2009)
14. K. Tanaka, A. Kunioks, Y. Sakai, Jpn. J. Appl. Phys. **8**, 681 (1969)
15. H. Kim, J. Horwitz, W. Kim, A. Makinen, Z. Kafafi, D. Chrisey, Thin Solid Films **420–421**, 539 (2002)
16. A. Khan Shamshad, F.S. Al-Hazmi, S. Al-Heniti, A.S. Faidah, A.A. Al-Ghamdi, Curr. App. Phys. **10**, 145 (2010)
17. A. Khan Shamshad, A.A. Al-Ghamdi, Mater. Lett. **63**, 1740 (2009)
18. A.A. Al-Ghamdi, A. Khan Shamshad, Physica B **404**, 4262 (2009)
19. X. Nie, S.H. Wei, S.B. Zhang, Phys. Rev. B **65**, 75111 (2002)
20. H. Ohta, M. Orita, M. Hirano, I. Yagi, K. Ueda, H. Hosono, J. Appl. Phys. **91**, 3074 (2002)
21. S.A. Knickerbocker, A.K. Kulkarni, J. Acad. Sci. Technol. A **14**, 1709 (1996)

22. J. Tauc, in *Amorphous and Liquid Semiconductors*, edited by J. Tauc (Plenum Press, New York, 1979), p. 159
23. R.R. Reddy, K. Rama Gopal, K. Narasimhulu, L. Siva Sankara Reddy, K. Raghavedra Kumar, C.V. Krishna Reddy, S.N. Ahmed, Opt. Mater. **31**, 209 (2008)
24. M. Anani, C. Mathieu, S. Lebid, Y. Amar, Z. Chama, H. Abid, Comput. Mater. Sci. **41**, 570 (2008)
25. D. Cody, *Semiconductors and Semimetals. Part B. Optical Properties*, vol. 21 (Academic Press, New York, 1984), p. 25
26. A. Anders, S.H.N. Lim, K.M. Yu, J. Andersson, J. Rosén, M. McFarland, J. Brown, Thin Solid Films **518**, 3313 (2010)
27. B. Roy, J.D. Perkins, T. Kaydanova, D.L. Young, M. Taylor, A. Miedaner, C. Curtis, H.-J. Kleebe, D.W. Readey, D.S. Ginley, Thin Solid Films **516**, 4093 (2008)
28. E. Bobeico, F. Varsano, C. Minarini, F. Roca, Thin Solid Films **444**, 70 (2003)
29. J. Ni, X. Zhao, X. Zheng, J. Zhao, B. Liu, Acta Mater. **57**, 278 (2009)